frontiers | Frontiers in Marine Science

TYPE Original Research
PUBLISHED 02 July 2024
DOI 10.3389/fmars.2024.1331333

OPEN ACCESS

EDITED BY
Hongbin Liu,
Hong Kong University of Science and Technology, Hong Kong SAR, China

REVIEWED BY
Alessandra Norici,
Marche Polytechnic University, Italy
Jun Sun,
China University of Geosciences, China

*CORRESPONDENCE
Aurélie Godrant
liligodrant@gmail.com
Brivaela Moriceau
brivaela.moriceau@univ-brest.fr

RECEIVED 31 October 2023
ACCEPTED 28 May 2024
PUBLISHED 02 July 2024

CITATION
Godrant A, Leynaert A and Moriceau B (2024) A study of the influence of iron, phosphate, and silicate in Si uptake by two *Synechococcus* strains. *Front. Mar. Sci.* 11:1331333. doi: 10.3389/fmars.2024.1331333

A study of the influence of iron, phosphate, and silicate in Si uptake by two *Synechococcus* strains

Aurélie Godrant[1,2*], Aude Leynaert[2] and Brivaela Moriceau[2*]

[1]AlgaeNutri, Brest, France, [2]Univ Brest, CNRS, IRD, Ifremer, LEMAR, Plouzane, France

We investigated the influence of iron (Fe), phosphate (PO_4), and silicic acid [$Si(OH)_4$] concentrations on Si uptake rate by two strains of *Synechococcus*. Growth rates, cellular biogenic silica (bSi), and silicon uptake rates were measured and compared. Both strains showed significant Si cellular contents varying from 0.04 47 fmol cell^{-1} to a maximum of 47 fmol cell^{-1}, confirming that the presence of Si in *Synechococcus* is a common feature of the genus but with strain specificity. Maximum Si cell contents were measured when Fe and P co-limited RCC 2380 growth (47 fmol Si cell^{-1}) and under -Fe-Si limitations (6.6 fmol Si cell^{-1}) for the second strain RCC 1084. Unambiguously, all conditions involving P limitations induced an increase in the Si uptake by the two *Synechococcus*. Moreover, RCC 1084 showed a relationship between Si cellular quota and growth rate. However, both strains also showed a clear impact of Fe concentrations on their Si uptake: Si quotas increased 1) under Fe limitation even without P co-limitation and 2) under simple Fe limitation for RCC 1084 and with Si co-limitations for RCC 2380. Both strains exhibited a behavior that has never been seen before with changing $Si(OH)_4$: concentrations of 150 µM of $Si(OH)_4$ negatively impacted RCC 2380 growth over 10 generations. Conversely, RCC 1084 was limited when $Si(OH)_4$ concentrations dropped to 20 µmol L^{-1}. Maximum *Synechococcus* Si uptake rates normalized to the organisms' size (7.46 fmol µm^{-3} day^{-1}) are comparable to those measured for diatoms and rhizarians. From our data, and using all the data available on *Synechococcus* Si content and Si uptake rates, their average concentrations for each Longhurst province, and existing descriptions of the dominant nutrient limitations and *Synechococcus* strain specificity, we estimated at the global scale that the annual bSi stock contained in *Synechococcus* is 0.87 ± 0.61 Tmol Si, i.e., around a quarter of the bSi stock due to diatoms. We also estimated that the global Si production due to *Synechococcus* could average 38 ± 27 Tmol Si year^{-1}, which is roughly 17% of the total global annual Si production.

KEYWORDS

iron, phosphorus, silicon, *Synechococcus*, Si uptake, global Si budget

Introduction

The ocean is an important climate regulator, absorbing about one quarter of anthropogenic carbon (C) through its physical and biological pumps. The biological carbon pump (BCP) intensity depends on several complex processes that challenge our capacity to quantify its impact (Siegel et al., 2023). Among these difficulties, we may cite the understanding of the contribution of the different groups of organisms (Benedetti et al., 2023). Diatoms are well-known actors of the BCP due to their diversity, size, and capacity to dominate high-latitude ecosystems: their heavy frustule of biogenic silica that ballasts them and their capacity to aggregate, two characteristics that increase their sinking toward deep layers (Tréguer et al., 2018). It appears that high-latitude ecosystems dominated by diatoms are efficient at exporting C, but the proportion of this exported C reaching sequestration depth, i.e., the transfer efficiency, is low. Conversely, large oligotrophic zones do not export much C to the top of the mesopelagic layer but are efficient at transferring it to sequestration depth (Henson et al., 2012). Moreover, small cells such as cyanobacteria may also be important contributors to the C export (Richardson and Jackson, 2007; De Martini and Neuer, 2016). Through their domination in oligotrophic waters, a large part of the ocean, models estimate that pico-phytoplankton may contribute for 46% of the C export (Letscher et al., 2023). One of these groups, *Synechococcus*, contributes to the total primary production as high as 30% in the subtropical North Atlantic (Duhamel et al., 2019) or 25% in Costa Rica upwelling (Muñoz-Marín et al., 2020), and their global contribution has been estimated using niche model to be 16.7% (Flombaum et al., 2013). Indeed, *Synechococcus* have a wide repartition zone and a small seasonality (Visintini and Flombaum, 2022). These traits may be attributed to high adaptability in order to grow at low nutrient concentrations, use mixotrophy, or change their pigment content (Flombaum et al., 2013; Grébert et al., 2018; Muñoz-Marín et al., 2020; Visintini et al., 2021; Visintini and Flombaum, 2022). Surprising most of the scientific community, *Synechococcus* has been found to accumulate Si at a level that cellular ratios of Si/S and Si/P approach those detected in diatoms from the same environment (Baines et al., 2012; Ohnemus et al., 2016; Wei et al., 2022; Churakova et al., 2023). Until now, the scientific community has been unable to identify physiological mechanisms requiring the assimilation of dissolved Si (Brzezinski et al., 2017) and, thus, to understand the implication of this accumulation on the processes driving the oceanic C and silicon cycles. While poorly constrained models predict that climate change may increase the global abundances of *Synechococcus* at the expense of diatoms, they will be favored by three main impacts: ocean acidification, warming waters, and decrease of nutrients (Marinov et al., 2013; Dutkiewicz et al., 2015; MaChado et al., 2019; Flombaum and Martiny, 2021). However, due to the lack of data and comprehensive processes, none of these models consider the implication of *Synechococcus* accumulating Si. Moreover, considering the predicted increase of nutrient limitation, one has to comprehend the *Synechococcus* Si uptake under different limitations. Previous study showed the implications of P in the Si absorption process by *Synechococcus*: Si uptake rates were inhibited after addition of PO_4 in the medium of laboratory cultures (Brzezinski et al., 2017), suggesting that Si would be transported by P transporters instead of P. However, this study also showed that addition of a mix of vitamins and metals in this culture increased the specific uptake rate of Si compared to control. Both these results, and unpublished data that we collected in our laboratory with *Synechococcus* cultures, lead us thinking that Fe plays an important role in Si uptake by these cyanobacteria.

Due to its extremely low concentration, iron (Fe) limits phytoplankton productivity in ~30% of the world's oceans, in the high-nutrient low-chlorophyll waters (Moore et al., 2013). Cyanobacteria have been proposed to possess a high cellular growth requirement for Fe as a vestige of the high availability of Fe in the ancient ocean: Brand's (1991) hypothesis was based on the much higher subsistence Fe/P requirements in six coastal and oceanic *Synechococcus* strains whose growth has been reduced to zero by Fe limitation in comparison to subsistence Fe/P values of eukaryotic algae. There is no evidence for potential direct effect on cyanobacterial growth due to interactions between Fe and P concentrations in the environment, but, as Fe is an important controlling factor for phytoplankton growth, it has a feedback effect on the P demand and potentially on Si absorption.

In the present study, we propose to examine the uptake of Si by two *Synechococcus* strains under various $Si(OH)_4$, PO_4, and Fe conditions to help understand the processes involved, the *Synechococcus* contribution to the global Si oceanic cycle and whether *Synechococcus* may be or become a competitor of diatoms for Si resources.

Materials and methods

Cultures

Two strains of *Synechococcus* were studied: *Synechococcus* RCC2380 (ROS8604 Syn Clonal) from the Roscoff Estacade from France (48.732001, −3.982762), and RCC1084 (WH5701) from the Long Island Sound in USA (41.074403, −73.071732). These strains were sampled in coastal areas, but they belong to two clades that are more widely distributed: the RCC2380 belongs to the clade I that is widely represented worldwide from the Arctic to the Antarctic and in the westerlies domains, and RCC1084 belongs to the clade 5.2 that is a more coastal *Synechococcus* also observed in the Antarctic ocean (Doré et al., 2022 and 2023).

Semi-continuous batch cultures were maintained in an incubator at 22°C under 12-h/12-h light/dark cycle with a light intensity of 100 µEinstein m^{-2} s^{-1}, in order to keep cultures in the exponential growth phase. Cultures were maintained in acid washed polycarbonate flasks, in a variation of the Aquil medium (Price et al., 1989) containing EDTA (5 µmol/L; Table 1). Various concentrations of Fe, $Si(OH)_4$, and PO_4 were tested as indicated in Table 2. Like for every semi-continuous culturing system, macronutrient concentrations were high compared to environmental conditions, to compensate for the lack of renewal in the system compared to *in situ* and due to the cell concentration in our cultures that were much higher than in the ocean. It is a well-known method that using higher nutrient concentrations in semi-continuous cultures helps keeping good ratios between micronutrient concentrations and control the limitations. Limitations were evidenced through a decrease of the growth rates (Figure 1).

All conditions were adapted for eight generations and maintained between 2 and 8 months. Each experiment was done on at least four

10.3389/fmars.2024.1331333

TABLE 1 Aquil medium recipe for salt and nutrients, according to Price et al. (1989), EDTA is used at a final concentration of 5 µmol/L to stabilize metal concentrations.

	Final concentration (mol/L)
Synthetic oceanic water	
NaCl	4.20×10^{-1}
KBr	8.40×10^{-4}
Na_2SO_4	2.88×10^{-2}
$NaHCO_3$	2.38×10^{-3}
KCl	9.39×10^{-3}
H_3BO_3	4.85×10^{-4}
NaF	7.14×10^{-5}
$MgCl_2$, $6H_2O$	5.46×10^{-2}
CaCl2, $2H_2O$	1.05×10^{-2}
SrCl2, $6H_2O$	6.38×10^{-5}
Nutrients	
NaH_2PO_4, $2H_2O$	2.00×10^{-5}
$NaNO_3$	8.84×10^{-4}
$Na2SiO_3$, $9H_2O$	1.50×10^{-4}
Trace metals	
$ZnSO_4$, $7H_2O$	4.00×10^{-9}
$MnCl_2$, $4H_2O$	2.30×10^{-8}
$CoCl_2$, $6H_2O$	2.50×10^{-9}
$CuSO_4$, $5H_2O$	9.97×10^{-10}
Na_2MoO_4, $2H_2O$	1.00×10^{-7}
Na_2SeO_3	1.00×10^{-8}
$KCr(SO_4)_2$, $12H_2O$	1.00×10^{-8}
Na_3O_4V	1.00×10^{-8}
$FeCl_3$, $6H_2O$	1.00×10^{-7}

TABLE 2 Concentrations of PO_4, $Si(OH)_4$, and Fe in Aquil for the different conditions studied in the present study.

Name	PO4 (mol/L)	Si(OH)4 (mol/L)	Fe (mol/L)
Control	2.00×10^{-5}	1.50×10^{-4}	1.00×10^{-7}
-Fe	2.00×10^{-5}	1.50×10^{-4}	1.00×10^{-8}
-P	2.00×10^{-6}	1.50×10^{-4}	1.00×10^{-7}
-Si	2.00×10^{-5}	2.00×10^{-5}	1.00×10^{-7}
-Fe-P	2.00×10^{-6}	1.50×10^{-4}	1.00×10^{-8}
-Fe-Si	2.00×10^{-5}	2.00×10^{-5}	1.00×10^{-8}
-Si-P	2.00×10^{-6}	2.00×10^{-5}	1.00×10^{-7}
-Si–Fe	2.00×10^{-5}	2.00×10^{-5}	1.00×10^{-9}

culture replicates. Flow cytometry was used to count the cells and check their physiological stability by following the relative size (FSC), relative complexity (SSC), and fluorescence (yellow and red fluorescence) every 3 days. Experiments and analyses were only done when the parameters stayed within 90% of their optimum value and at the exponential phase. Growth curves and rates were determined every three days from these counts.

For a more fluid reading, we indicated in the rest of the text the PO_4 and $Si(OH)_4$ medium concentrations as follows: "P" and "Si."

Si-cellular quotas

Hereafter, Si-cellular quotas are understood as being the total amount of Si coming from the cells (including particulate and soluble Si). Si-cellular quotas were measured on 10 mL to 15 mL of cultures that were filtered on 0.4-µm pores polycarbonate filters. Filters were rinsed with synthetic oceanic water (SOW) (Price et al., 1989) to wash away adsorbed $Si(OH)_4$ and placed in 15-mL tubes for drying at 60°C in an oven. Cells were digested in NaOH (0.2 mol/L) at 90°C in a water bath for 4 h (Moriceau et al., 2007). After cooling, the digestates were acidified with HCl (1 mol L^{-1}), and the tubes were centrifuged at

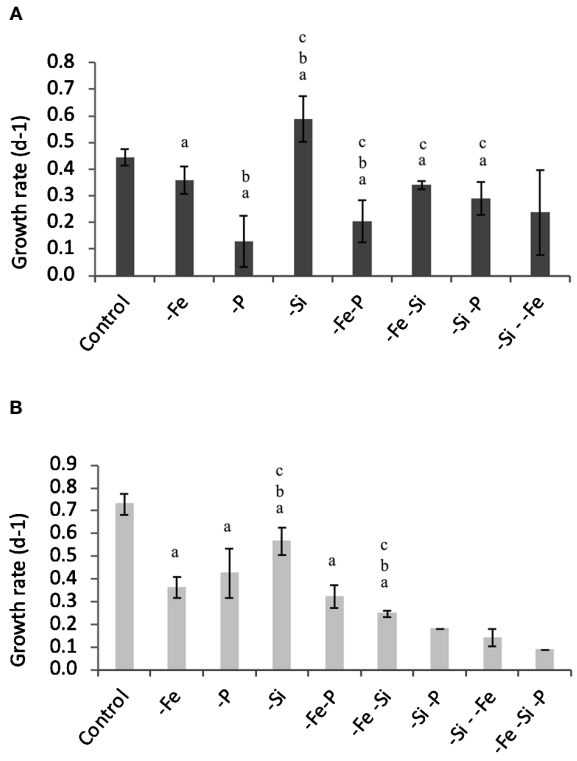

FIGURE 1
Specific growth rates of cultures RCC 2380 **(A)** and RCC 1084 **(B)** exposed to different concentrations of Fe, PO_4, and $Si(OH)_4$. Error bars represent standard deviations. Tamhane test with $p < 0.05$ was indicated in the graph with "a" for treatments significantly different from control, with "b" for treatments significantly different from -Fe, and with "c" for treatments significantly different from -P. For RCC 2380 treatment -Si–Fe and for RCC 1084 treatments -Si-P, -Si–Fe and -Fe-Si-P, too few data were obtained and statistical analyses were not possible.

3,000 rpm for 5 min. The supernatant was analyzed for silicates by colorimetry using an AutoAnalyzer (Bran and Luebbe Technicon Autoanalyzer, accuracy of 0.1%) according to the protocol optimized by Aminot and Kérouel (Aminot and Kérouel, 2007).

Rate of Si uptake

Biogenic Si uptake rates (ρSi) were measured by the ^{32}Si method (Tréguer et al., 1991; Leynaert et al., 1996). Culture flasks of 15 mL to 20 mL were spiked with 650 Bq of radiolabeled ^{32}Si-silicic acid solution with a specific activity of 18.5 kBq µg Si^{-1}, resulting in an increase in silicic acid concentration no greater than 0.1 µmol L^{-1}. Samples were then incubated in the laboratory for 24 h. After incubation, samples were filtered onto 0.6-µm Nucleopore polycarbonate filters and rinsed twice with filtered seawater to wash away non-particulate ^{32}Si. Each filter was then placed in a 20-mL polypropylene scintillation vial. The activity of ^{32}Si in the samples was determined 12 months later, allowing ^{32}Si and its daughter isotope ^{32}P to return to secular equilibrium. Samples were assayed using a scintillation counter Wallac Model 1414. The silicic acid uptake rate (ρ_{Si}, in µmol L^{-1} h^{-1}) was calculated as follows:

$$\rho_{Si} = \frac{A_f}{A_i} \times [Si(OH)_4] \times \frac{1}{\Delta t}$$

where $[Si(OH)_4]$ is the silicic acid concentration of the sample (µmol L^{-1}); A_i and A_f are the initial and final activities of the sample (cpm), respectively; and Δt is the incubation time (in hours). Triplicate 60-min counts were performed on each sample. Counting precision (95% confidence interval) was< ± 5%. The background for the ^{32}Si radioactive activity counting was 8 cpm. Samples for which the measured activity was less than three times the background were considered to lack Si uptake.

Statistical analysis

Statistical analyses were conducted on the growth rates and the Si-cellular quotas using one-way ANOVA. When ANOVA showed significance, we applied a *post-hoc* Tamhane test adapted to unequal variance to determine which of the treatment pairs are significantly different (Figures 1, 2).

For the analysis of the results displayed in Figures 3A, 4C, we conducted linear regressions and obtained the Pearson's correlation coefficients for each of them with $p< 0.05$.

Results

Effect of Fe, PO_4, and $Si(OH)_4$ concentrations on specific growth rates

We obtained growth rates for the two strains for each culturing condition described in Table 2. Results are indicated in Figures 1A, B. Firstly, the decrease in P and/or Fe concentrations in the culture media induced significant lower growth rates for both RCC 2380 and RCC 1084. When P concentration decreased from 20 µmol L^{-1} to 2 µmol L^{-1}, the growth rate was reduced from 0.44 day^{-1} to 0.1 day^{-1} for RCC 2380 and from 0.73 day^{-1} to 0.4 day^{-1} for RCC 1084. When Fe concentration was lowered from 100 nmol L^{-1} to 10 nmol L^{-1}, the growth rate significantly decreased for both RCC 2380 and RCC 1084 from 0.44 day^{-1} to 0.36 day^{-1} and from 0.73 day^{-1} to 0.36 day^{-1}, respectively. When $Si(OH)_4$ concentration decreased from 150 µmol L^{-1} to 20 µmol L^{-1}, RCC 2380 growth rate increased from 0.44 day^{-1} to 0.59 day^{-1}, whereas RCC 1084 growth rate decreased from 0.73 day^{-1} to 0.57 day^{-1}. Secondly, the maximum decrease in RCC 2380's growth rate was achieved when only P concentration was lowered. None of the additional limitations showed any further reduction in growth rate, even when co-limited with P (-Fe-P and -Si-P). In contrast, RCC 1084 growth rates were systematically more impacted when more than one nutrient was limiting, with values lower than 0.3 day^{-1} and down to 0.1 day^{-1} when Fe, Si, and P concentrations were simultaneously reduced in the culture media. However, the growth rate decrease observed for -Fe-P co-limitation was not significantly different from those measured for Fe and P simple limitation.

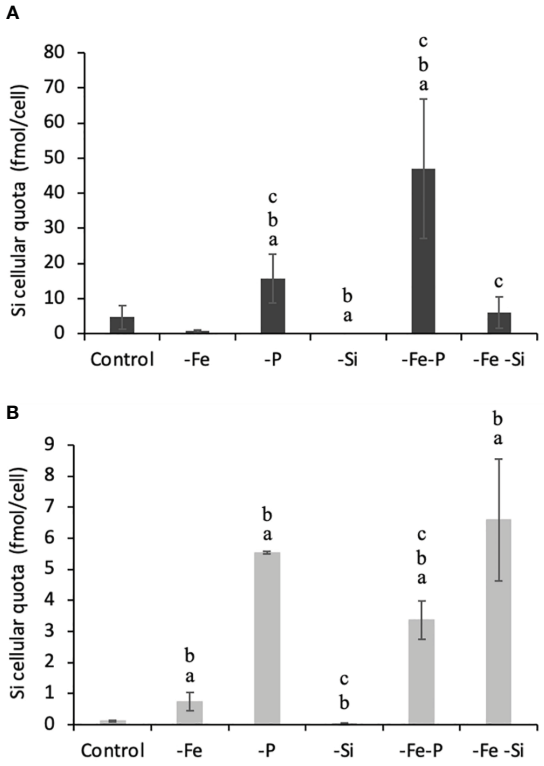

FIGURE 2
Biogenic silica cell content varying with culturing conditions for RCC 2380 **(A)** and RCC 1084 **(B)**. Error bars represent standard deviations. $p< 0.05$, significantly different from control marked with a "a," test significantly different from -Fe marked with a "b," and significantly different from -P marked with a "c.".

Effect of $Si(OH)_4$, Fe, and PO_4 concentrations on Si cellular quotas

The two strains were examined for their Si quotas as a function of nutrients variations as described in the method. Figure 2

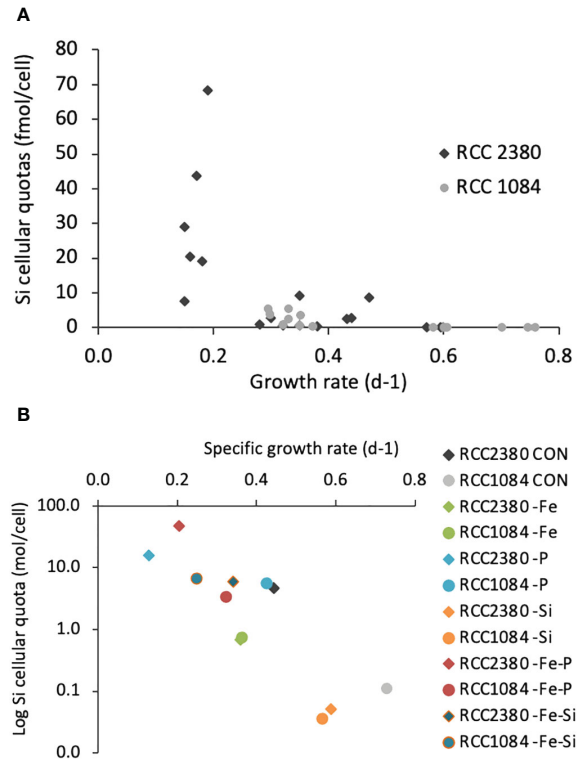

FIGURE 3
Si cellular quotas as a function of specific growth rates of RCC 2380 and RCC 1084 in all various media conditions. All data are indicated in **(A)**, and average results for each medium condition are indicated in **(B)**.

represents cellular Si quotas for the two strains, with variable P, Fe, and Si concentrations. RCC 2380 had Si quotas ranging from 0.05 fmol cell^{-1} to 47 fmol cell^{-1}, whereas RCC 1084, starting from a similar value of 0.04, only reached maximum Si quotas of 6.6 fmol cell^{-1}: RCC 2380 had a maximum Si quota seven times higher than that of RCC 1084. In our conditions, the maxima were reached for the -Fe-P conditions for RCC 2380.

Considering simple and co-limitation of P, both -P and -P-Fe significantly increased bSi as they were multiplied by 3 to 50 for both strains compared to controls. P limitation strongly increased Si quotas, an effect that is enhanced for Fe co-limitation in RCC 2380.

When Fe concentration was reduced from 100 nmol L^{-1} to 10 nmol L^{-1}, both strains exhibited opposite trends for simple Fe limitation: RCC 2380 decreased its Si content from 4.74 fmol cell^{-1} to 0.69 fmol cell^{-1}, whereas RCC 1084 increased it from 0.11 fmol cell^{-1} to 0.73 fmol cell^{-1}. For both strains, adding P to Fe limitation enhanced Si quotas compared to both control and -Fe. Moreover, -Fe-Si exhibited higher Si quotas than -Si for RCC 1084.

When $Si(OH)_4$ concentration was reduced from 150 µmol/L to 20 µmol/L, Si quota slightly decreased for RCC 1084 from 0.11 fmol cell^{-1} to 0.04 fmol cell^{-1}, whereas it decreased by two orders of magnitude for RCC 2380: from 4.74 fmol cell^{-1} to 0.05 fmol cell^{-1}. However, as described earlier, when both Fe and Si were reduced, the two strains increased their Si quota compared to -Si: from 0.05 fmol cell^{-1} to 5.98 fmol cell^{-1} for RCC 2380 and from 0.04 fmol cell^{-1} to 6.59 fmol/cell^{-1} for RCC 1084.

We investigated the relationship between growth rates and Si-cellular quotas for both strains, and the results are presented in Figure 3. Linear regressions give an r-value of −0.60 for RCC 2380 and −0.71 for RCC 1084 ($p< 0.05$), which means that the correlation between Si-cellular quotas and growth rates is negative (bSi decreases when growth rate increases) and that it is stronger for RCC 1084 than for RCC 2380. However, the coefficients being not very high, they show that the correlation between bSi and growth rates is not very strong.

Displaying the average value of each condition in Figure 3B, this indicates the differences between the two strains: the correlation between growth rate and Si-cellular quotas was extremely similar for the two strains only for -Si and -Fe conditions. All other conditions were very different.

Si uptake rates

The Si uptake rates were measured as indicated in the method for the control, -Fe, -P, -Si, and -P-Fe conditions for both strains and -Fe-Si for RCC 2380 (Figure 4).

Si uptake rates of RCC 2380 (Figures 4A1, A2) varied between 0.01 fmol cell^{-1} day^{-1} for -Si and 21.4 fmol cell^{-1} day^{-1} for -Fe-P. Meanwhile, for RCC 1084 (Figures 4B1, B2), it varied between 0.002 fmol cell^{-1} day^{-1} for -Si and 2 fmol cell^{-1} day^{-1} for -P. As a global observation, RCC 1084 Si uptake rates were one order of magnitude lower than RCC 2380, as for the Si quotas. In general, we observe that the variations between conditions have similar trends than the Si quotas: linear regression gave an r-value of 0.99 ($p< 0.05$), which shows a very good correlation between Si-cellular quotas and Si uptake rates (Figure 4C).

Considering variations in Si uptake rates with varying Si medium conditions, RCC 2380 control exhibited a rate of 0.92 and fmol cell^{-1} day^{-1}, but it was close to the detection limit for the -Si and -Si -Fe conditions with rates of 0.010 fmol cell^{-1} day^{-1} and 0.007 fmol cell^{-1} day^{-1}, respectively. For RCC 1084, both the control and the -Si condition were close to the limit of detection with rates of 0.020 fmol cell^{-1} day^{-1} and 0.002 fmol cell^{-1} day^{-1}, respectively.

For both strains, Si uptake rates were higher for all the -P simple and co-limitations compared to control. We can see differences between RCC 2380 and RCC 1084 for -Fe limitations: RCC 2380 -Fe uptake rate decreased compared to the control; -Fe-P was higher than the control and even higher than the -P condition; whereas, for RCC 1084, -Fe and -Fe-P conditions showed both higher Si uptake rates than the control.

These data represent specific uptake rates between 0.0003 h^{-1} and 0.0195 h^{-1}, which we can compare with the rates of 0.007 h^{-1} to 0.101 h^{-1} found in previous study (Brzezinski et al., 2017).

Discussion

Regulation of *Synechococcus* Si uptake by dissolved Fe, Si, and P concentrations

In the present study, we analyzed how the capacity to uptake Si of two strains of the genus *Synechococcus* from two distinct clades

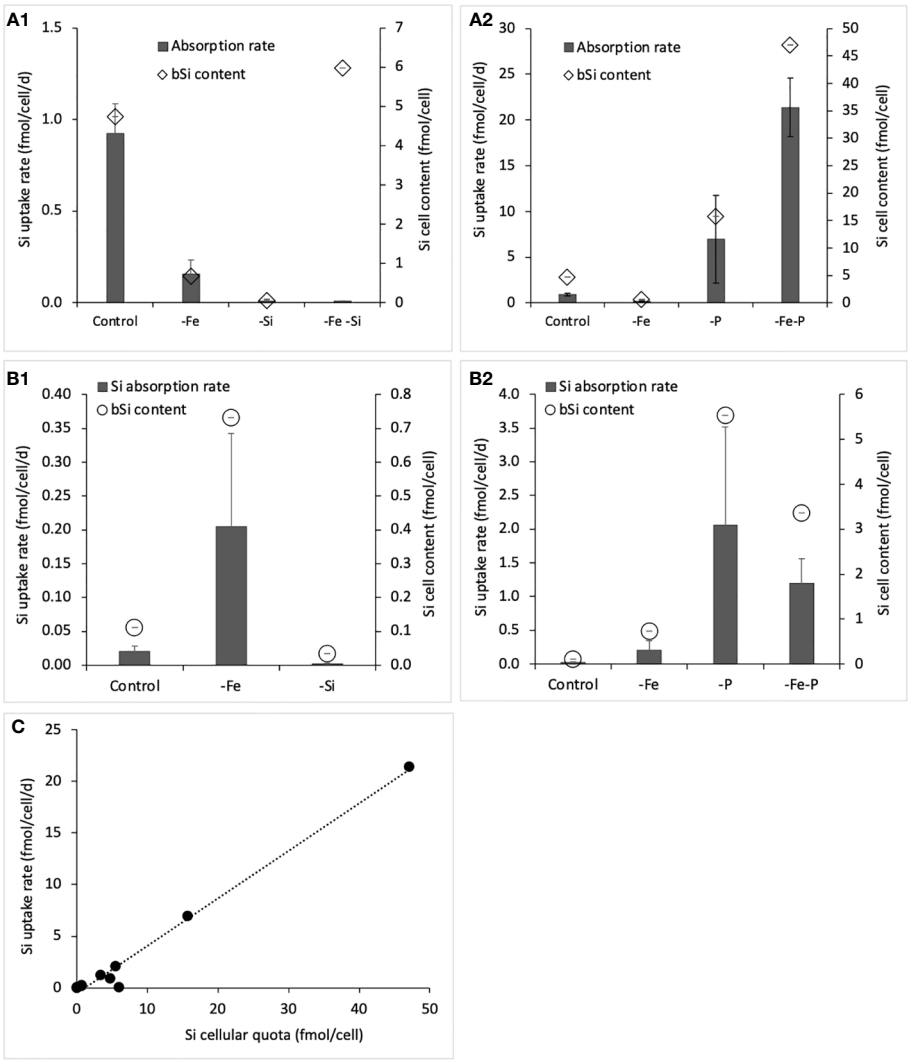

FIGURE 4
Silicic acid uptake rates and Si cellular quotas (bSi) for **(A1)**: RCC 2380 cultured in control conditions vs. Fe simple limitations, low silicic acid concentration, Fe limitations combined to low silicic acid concentrations; **(A2)** RCC 2380 cultured under no limitations vs. Fe and P simple and co-limitations; **(B1)** RCC 1084 cultured under no limitations vs. Fe and Si simple limitations; **(B2)** RCC 1084 cultured under no limitations vs. Fe and P simple and co-limitations. Panel **(C)** compares Si cellular quotas and Si uptake rates for both strains.

(RCC2380, clade I and RCC1084, clade 5.2) may be modified by changing Fe, P, and Si concentrations. Observations of Si accumulation inside *Synechococcus* cells are challenging and must be conducted under strict control of the pH. We took care to maintain pH, i.e., remaining< 8.3 and Si uptake rate obtained in our study were truly biotic processes and not abiotic Si precipitation (Nelson et al., 1984). We undertook our experiments using the Aquil medium, allowing us to control every single nutrient, metal, and vitamin and to provide stable conditions. Nutrient limitations were established by the decrease in the growth rate measured for RCC 2380 and RCC 1084. With this definition in mind, all conditions where growth rate decreased (stable over 10 generations) implied an efficient limitation.

For RCC 2380, the decrease in growth rate between -Si and control suggested a toxic effect of $Si(OH)_4$ on *Synechococcus* growth. The fact that $Si(OH)_4$ concentrations modified the growth rates of both strains is surprising given that *Synechococcus* is known to lack an obligate need for silicon (Brzezinski et al., 2017) and seems insensitive to potential toxic effects of high $Si(OH)_4$ concentrations (Tostevin et al., 2021). However, considering 1) the lower RCC 2380 growth rates in all conditions compared to -Si and especially the increase in growth rate for -Si compared to the control and for -Si-P compared to -P and 2) taking into account that, for RCC 1084, all the conditions, including -Si, have lower growth rates than the control, suggest strain-dependent toxicity effect of high $Si(OH)_4$ concentrations. Our two strains are coastal and used to meet large variations in $Si(OH)_4$ concentrations. Indeed, RCC 2380 is from the Manche, whereas RCC 1084 is from Long Island Sound a semi-enclosed Bay in the USA. By comparison, the strain from the study by Tostevin is pelagic and comes from the Caribbean Sea. At the Roscoff site, $Si(OH)_4$ reaches a maximum of 6 µmol L^{-1} in winter and a minimum of 1.5 µmol L^{-1} in June (Sournia and Birrien, 1995;

Cariou et al., 2004). The ecosystem encounters silicate limitation with respect to nitrate during winter and spring (DIN: DSi< 1) and nitrate limitation during summer. In long Island Sound, $Si(OH)_4$ varies annually from 40 µmol L^{-1} to 1.6 µmol L^{-1} in spring and summer (Gobler et al., 2006; George et al., 2015), and phytoplankton is Si limited with respect to N in summer. In our study, $Si(OH)_4$ concentrations had a strain-specific impact on *Synechococcus* growth rate. RCC 2380 was negatively affected by the highest $Si(OH)_4$ concentrations, and its growth rate significantly increased when $Si(OH)_4$ concentrations decreased from 150 µmol L^{-1} to 20 µmol L^{-1}. This trend can be seen comparing four culturing conditions: control vs. -Si and -P vs. -P-Si. On the contrary, RCC 1084 growth rate significantly decreased when $Si(OH)_4$ concentration was reduced, as seen comparing control vs. -Si, -P vs. -P-Si, and also -Fe vs. -Fe-Si.

Brzezinski and collaborators (2017) also studied the growth rates of six *Synechococcus* clones (including the WH5701 = RCC 1084 in the present study), under varying $Si(OH)_4$ medium concentrations of 1 µmol L^{-1}, 60 µmol L^{-1}, or 120 µmol L^{-1}, and found no significant differences in their growth rates. Our cultures were maintained in a completely synthetic and controlled Aquil medium containing PO_3 (20 µmol L^{-1}) and Fe (100 nmol L^{-1}), whereas Brzezinski's cultures were maintained in a medium made of aged 0.2-µm filtered surface Sargasso Sea water with f/2 medium constituents and containing added PO_3 (36 µmol L^{-1}) and Fe (11.7 µmol L^{-1}). Differences in growth rates between our study and Brzezinski et al. (2017) might stem from medium differences and more specifically metals concentrations. Our study highlights the potential role of metal and, specifically, Fe concentrations on Si uptake by *Synechococcus*. Moreover, these results indicate strain-dependent discrepancies.

The range of Si uptake rates obtained in our study (0.04 fmol Si $cell^{-1}$ to 47 fmol Si $cell^{-1}$ and 0.003 fmol μm^{-2} to 4 fmol μm^{-2}) confirms those measured during field observations from the equatorial Pacific, the Sargasso Sea, and laboratory experiments (0.0006 fmol Si $cell^{-1}$ to 4.7 fmol Si $cell^{-1}$; Baines et al., 2012; Ohnemus et al., 2016; Brzezinski et al., 2017, 2018; Krause et al., 2017; Wei et al., 2022). *Synechococcus* cells contain significant but variable amounts of Si, with cellular Si quotas staying low compared to the most studied silicifiers, i.e., diatoms, cultivated in different nutrients' availability (20 pmol Si $cell^{-1}$ to 225 pmol Si $cell^{-1}$; Martin-Jézéquel et al., 2000; Marchetti and Harrison, 2007; Boutorh et al., 2016). Si cellular quota in our laboratory was more stable than in field samples, where Si per cell could vary at least by an order of magnitude among cells from a single sample. However, many strains coexist *in situ*, and we observed large strain-specific responses to nutrient conditions, probably due to their high capacity to adapt to their environment.

The first hypothesis proposed to explain the mechanisms of Si accumulation by *Synechococcus* (Brzezinski et al., 2017) suggested two possibilities: 1) a lack of selectivity in the transport of PO_4 through the cell membrane, leading to $Si(OH)_4$ molecules being transported instead of PO_4 inside the cell and 2) passive diffusion of $Si(OH)_4$ into the cell, with both mechanisms being enhanced by decreased growth rates, allowing more $Si(OH)_4$ accumulation inside the cells.

A global analysis of RCC 1084 suggests that most limitations, except -Si, simultaneously decreased cell growth and increased Si cell content supporting Brzezinski's hypothesis. Indeed, for RCC 1084, Figure 3 shows that Si cellular quota is dependent upon growth rate with a R^2 of 0.65. However, such a growth effect is not clear for RCC 2380 with a R^2 of only 0.29. PO_4 concentration and Si:P ratio appear to be determinant parameters for Si uptake by *Synechococcus*, as suggested by Brzezinski's study. Additionally, our results indicate the involvement of Fe in Si uptake by some strains of *Synechococcus*. For *Synechococcus*, -Fe-Si induced a higher Si quota than -Si and -Fe alone despite higher growth rate for RCC 2380. The interaction between P and Fe metabolisms and Si accumulation in *Synechococcus* is evident, suggesting a complex role of Fe in Si uptake, possibly, but not exclusively, through implications of Fe in the PO_4 transporters, albeit differently between strains. The significantly higher Si quotas of cells grown under -Fe-Si compared to -Fe, challenge the theory of passive silicon diffusion through cell membranes, especially considering RCC 2380.

In their study, Marron et al. (2016) suggested that the SIT-L in *Synechococcus* may be to avoid $Si(OH)_4$ toxicity in ancient oceans, potentially implying that Si cellular quotas may be more controlled in organisms that have the presence of this Si transporter. RCC 2380 and RCC 1084 are positioned at the two extreme opposite ends of the phylogenetic tree drawn by Doré and collaborators (Doré et al., 2020), suggesting different evolutionary histories and adaptations. RCC 1084 likely appeared much earlier than RCC 2380, possibly before 878 My ago (Doré et al., 2020), when Si concentration in the world oceans was above 1 mol L^{-1}. We do not have the timing for RCC 2380 occurrence, but it appeared much later than 250 My ago, when Si in the ocean waters started to significantly decrease (Marron et al., 2016). The relatively low gene fixation rate observed by Doré et al. (2020) implies that flexible genes that are fixed within a clade (i.e., clade-specific genes) were gained tens of millions of years ago and thus might be more reflective of past selective forces than of recent adaptation to newly colonized niches. We could not find such SIT-L genes in the published genomes of RCC 2380 and RCC1084, and further exploration is needed.

Another hypothesis from Tang et al. (2014) suggests that silicon may accumulate and precipitate on the cell membrane of dead *Synechococcus*. If we consider that the growth rate may be an indicator of the number of dead *Synechococcus* in the culture, then, indeed, low growth rates may involve more dead cells and following the Tang's hypothesis, more silicon accumulating on the membrane of the cells. However, our study showed that growth conditions modified Si content without affecting growth rate, indicating a more complex relationship. For example, -Fe and -Fe-P conditions for RCC 2380 and -Fe, -P, and -Fe-P conditions for RCC 1084 led to similar growth rate but different Si cellular quotas and Si uptake rates.

Overall, our study sheds light on the regulation of Si uptake in *Synechococcus*, emphasizing the importance of Fe, Si, and P concentrations and highlighting strain-specific responses, which contribute to our understanding of the ecological roles of these microorganisms in the oceanic ecosystem. However, the mechanisms explaining these links still need further exploration.

In comparison, the metabolic response of diatoms to Fe limitation is also species specific (Cohen et al., 2017), leading to different consequences for Si accumulation with increasing silicification and frustule mechanical strength for some species (Wilken et al., 2011), no change of Si cellular quotas (Brzezinski et al., 2011) or decreasing silicification in others (Boutorh et al., 2014; Lasbleiz et al., 2014). Although Fe may be involved in Si homeostasis in diatoms (Petrucciani et al., 2022), the link between Fe availability and diatom Si metabolism remains misunderstood despite the fact that diatoms are the most studied silicified marine organisms.

Si uptake rates measured in our study are surprisingly comparable to those measured for diatoms and rhizarians, which play an important role in the Si cycle (Biard et al., 2018; Llopis Monferrer et al., 2020; Tréguer et al., 2021). In our study, Si uptake rates varied from 0.01 to 21 fmol cell^{-1} day^{-1}. By comparison, diatoms have Si uptake rates ranging from 1 to 21,000 fmol cell^{-1} day^{-1}, and rhizarians from 170,000 to 2,000,000 fmol cell^{-1} day^{-1} (Figure 5). Normalizing adsorption rates to biovolume shows similar Si uptake rates between the three silicifiers: 7.46 fmol µm^{-3} day^{-1} for rhizarians, 82.03 fmol µm^{-3} day^{-1} for diatoms, and 55.7 fmol µm^{-3} day^{-1} for *Synechococcus*. In the world ocean, diatoms uptake varies from 0.14 in the North Atlantic Tropical Gyre (Poulton et al., 2006; Tréguer et al., 2021) to a maximum of 202 mmol Si m^{-2} day^{-1} in the upwelling of California (Brzezinski et al., 1997; Tréguer et al., 2021). With a global average cell concentrations of 4 × 10^4 cells mL^{-1} and an average depth of 80 m (Visintini and Flombaum, 2022) cyanobacteria may uptake up to 22 mmol m^{-2} day^{-1} under P limitation and 68 mmol m^{-2} day^{-1} under P and Fe co-limitation. This renders *Synechococcus* real competitors of diatoms for $Si(OH)_4$ resource in the environment especially in zones encountering P and Fe limitations. Whereas P mostly is a secondary limiting nutrient and -P-Fe co-limited zones are scarce in the global ocean, Fe limitation concerns almost a third of the world ocean (Browning and Moore, 2023).

In conclusion, our study highlights the complex interplay between Fe, P, and Si concentrations in regulating Si uptake by *Synechococcus*, with strain-specific responses indicating the need for further research to elucidate the underlying mechanisms and ecological implications.

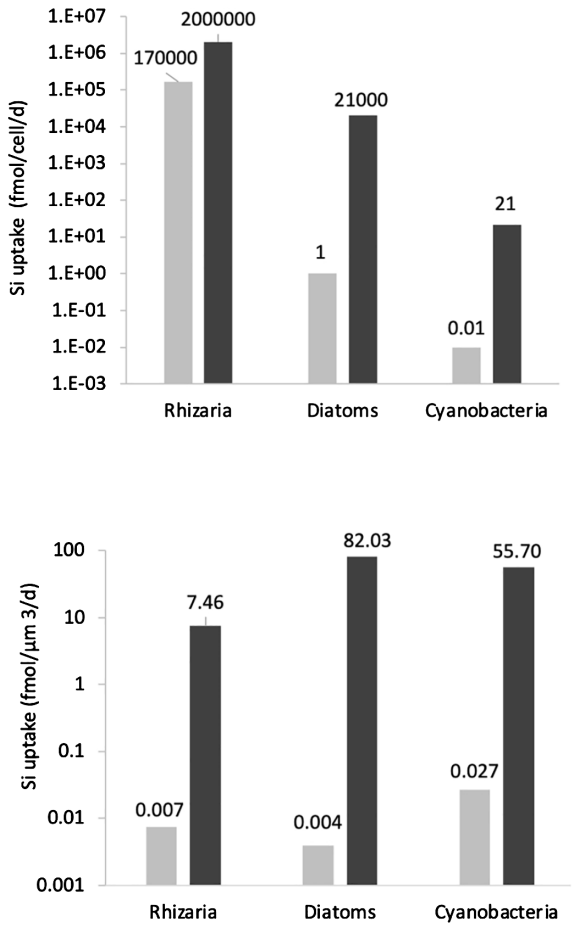

FIGURE 5
Global comparison of Si uptake rates between Rhizarians (Llopis Monferrer, 2020), Diatoms (Llopis Monferrer, 2020), and Cyanobacteria (present study). The first panel represents the Si uptake in fmol/cell/day, whereas, for the second panel, data were corrected with cell volumes and are presented in fmol/µm^3/day. Light gray bars represent the minimum values, and dark gray bars represent the maximum values found.

Meanings for the environment

Synechococcus dominate in oligotrophic waters. Meanwhile, their abundance is quite constant everywhere and throughout the year varying around 4×10^4 cells mL^{-1} with a global yearly abundance between 6.1 and 6.9×10^{26} cells (Visintini et al., 2021; Visintini and Flombaum, 2022). At the global scale, their seasonal variability is 15% (Visintini and Flombaum, 2022), and their concentration increases with temperature (Li, 1998). Spatially, their abundance is maximum in the westerlies winds domain and the trade winds domain defined by Longhurst (Longhurst et al., 1995) with a light decrease in cell abundance around 30° N and S and a minimum in the polar systems (Visintini et al., 2021; Visintini and Flombaum, 2022). The study by Baines and coworkers (2012) revealed for the first time that *Synechococcus* cells may contain Si in non-negligible amount, opening an interesting question on their potential contribution to the Si cycle. However, small diatoms of size similar to that of *Synechococcus* grow in similar locations than *Synechococcus* (Leblanc et al., 2018), which create difficulties to measure *in situ* the *Synechococcus* contribution to Si production, underlying the need to use process studies to evaluate their importance in the dynamics of the Si cycle.

Using a method similar to Tréguer et al. (2021), we estimated *Synechococcus*' global contribution to the Si cycle (Supplementary Materials). The annual average of the bSi standing stock related to *Synechococcus* is 0.87 ± 0.61 Tmol Si. To estimate the variability, we used the maximum standard deviation found in our experimental estimation of the Si quotas, which is smaller than *in situ* variability between cells that may be from different clades and reach more than 200% (Baines et al., 2012; Wei et al., 2022). Moreover, we could not consider seasonal variations of the clade dominance that seems to emerge from the different studies described in Table 3. This estimate is about an order of magnitude higher than the 0.05–0.09 Tmol-Si estimated from *in situ* data and Si/C quotas by Wei et al. (2022). By mean of comparison, rhizarians' Si standing stocks have been estimated to range from 0.08 to 5.25 Tmol Si by Biard et al. (2018) and between 0.07 and 0.72 Tmol Si by Llopis Monferrer et al. (2020) using a global ocean surface area of 328,106 km^2. Diatoms stay the main contributors of the pelagic stocks with 2–4 Tmol of Si (Leblanc et al., 2012). *Synechococcus* may contribute up to 20% of the total bSi pelagic stocks estimated here as the sum of the Si stocks constituted by the three silicifiers mentioned above.

In the revised Si budget made by Tréguer and co-workers, the annual production of biogenic silica at the global scale is 255 ± 52 Tmol $year^{-1}$, with most attributed to diatoms. However, in some region of the ocean (oligotrophic gyres), the contribution of the< 3-µm-size fraction, where *Synechococcus* fall, may reach up to 55% of the Si production (Krause et al., 2017). This production has been attributed to *Synechococcus* by the authors, but this is debated in Leblanc et al. (2018) as nano-diatoms may also be responsible for part of the Si production by small size organisms. On the other side, Wei and collaborators estimated the global annual Si production in the surface ocean due to picocyanobacteria would reach 45% (Wei et al., 2023). Si production is generally measured *in situ* on pelagic communities belonging to the > 0.45–0.6µm size fraction. With cell diameter varying between 0.8 µm and 3 µm and length above 1 µm, we may consider that *Synechococcus* contribution is included in the global Si budget. With this consideration in mind, the global annual Si production of 38 ± 27 Tmol Si $year^{-1}$ calculated in this study corresponds to a contribution of 17% of the total Si production. Acknowledging the high uncertainty, it is interesting to note that this is not so far from the 16.7% contribution to the C production estimated from niche model by Flombaum and collaborators (2013). This contribution shows strong spatial disparities, with a global 93% of the Si production attributed to *Synechococcus* in the Westerlies winds but only 10% in trade winds domain. Surprisingly, their contribution to the Southern Ocean may reach half of the Si production, most probably due here to the high cell abundance found by Visintini' study in the SANT and SSTC regions together with Fe limitations. Please note that, in this Southern region, the cellular Si quotas used to calculate the contribution of *Synechococcus* were not from our study. Despite uncertainties and strain differences in Si metabolisms, *Synechococcus*' contribution to the Si cycle, especially in oceanic regions like the westerlies or the Southern Ocean, is significant. With predicted increases of *Synechococcus* growth in future oceans, their role as actor in the Si cycle deserves to be taken into consideration with an urgent need to understand the mechanisms at stake.

Conclusions

The mechanisms governing Si accumulation in *Synechococcus* are complex and strain-specific, extending beyond the previously suggested factors of non-specific PO_4 transporters, $Si(OH)_4$ diffusion, and growth effects. Our study reveals that *Synechoccocus* Si metabolism is strain specific and that 1) Fe is involved in Si cellular accumulation but Fe limitation consequences on Si quotas are strain specific; 2) our *Synechococcus* strains revealed to be sensitive to Si $(OH)_4$ concentrations in their environment with opposite results, with one of them being negatively affected and the other one being positively affected by high $Si(OH)_4$ concentrations; and 3) Si cellular accumulation can increase or decrease even when $Si(OH)_4$ concentration in the medium decreases. Neither RCC 2380 nor RCC 1084 genomes contain identified SIT-L genes that could explain Si uptake by *Synechococcus*, underscoring the need for further laboratory experiments to explore additional nutrients and genetic factors influencing Si uptake. Not only the physiological mechanisms but also the consequences of this misunderstanding capacity of *Synechococcus* to accumulate Si need to be comprehended if we want to better predict the future of the Si cycle and of the BCP.

Overall, our study suggests a complex interplay between nutrient availability, particularly P and Fe, and Si uptake in *Synechococcus*, with strain-specific responses and potential ecological implications for nutrient cycling in the ocean.

Several questions remain unanswered, including the implications of *Synechococcus* Si accumulation for sinking and export, trophic interactions, and competition with diatoms. Future research perspectives may involve studying a larger

TABLE 3 *Synechococcus* contribution to the Si global oceanic cycle: review of the Supplementary Materials.

	Synechoccocus							Diatoms	Global Si cycle			Rhizarians	
	Average *Synechococcus* abundance		Ocean surface	Qsi	bSi	PbSi		bSi stocks	Surface used for diatom calculation	PbSi		bSi	PbSi
	10^4 cells/mL	10^{24} cells	10^6 km^2	fmol Si/cell	10^{10} mol Si	10^{12} mol an^{-1}	mol m^{-2} an^{-1}	mol Si	10^6 km^2	10^{12} mol an^{-1}	mol m^{-2} an^{-1}	mol Si	mol an^{-1}
Coastal	2.26	67.81	34.35	1.14	3.99	3.27	0.10		37	138.04	3.73		
Westerlies winds domain	2.51	248.89	132.97	3.18	81.59	38.02	0.29		129.9	29.65	0.23		
Trade winds domain	2.72	580.79	139.90	3.18	6.74	5.02	0.04		139.9	50.42	0.36		
Polar	0.63	9.26	20.78	3.19	3.06	1.50	0.07		53.98	66.83	1.24		
Global Ocean	2.27	648.43	328.00		95.38	47.80	0.15	2–4 × 10^{12}	360.78	284.93	0.79	0.66–7.22 × 10^{11}	2–58 × 10^{12}
Total Arctique	0.30	0.40	1.66		0.00	0.00	0.00		14	1.42	0.10		
Total Atlantique	2.20	151.12	74.15		15.92	15.48	0.21		86	21.50	0.25		
Total Océan Indien	2.88	107.81	45.38		0.74	0.27	0.01		54	37.19	0.69		
Total Pacifique	2.43	313.33	148.92		20.86	15.18	0.10		134	145.74	1.09		
Total Antarctique	1.26	75.78	57.89		57.85	16.87	0.29		73	42.76	0.59		
Global Ocean	1.81	648.43	328.00		95.37	47.80	0.15	2–4 × 10^{12}	361	248.61	0.69	0.66–7.22 × 10^{11}	2–58 × 10^{12}

For the purpose of comparison, data for diatoms and rhizarians are also provided in the table. Diatoms' bSi standing stock is sourced from Leblanc et al. (2018), whereas data on total Si production are obtained from Tréguer et al. (2021). Data for rhizarians are sourced from Llopis Monferrer et al. (2020).

10.3389/fmars.2024.1331333

number of *Synechococcus* strains coming from various clades to elucidate global physiological characteristics and specific habitat preferences.

Data availability statement

The original contributions presented in the study are included in the article/Supplementary Material. Further inquiries can be directed to the corresponding authors.

Author contributions

AG: Conceptualization, Formal analysis, Funding acquisition, Investigation, Methodology, Validation, Writing – original draft, Writing – review & editing. AL: Formal analysis, Methodology, Writing – original draft, Writing – review & editing. BM: Conceptualization, Formal analysis, Funding acquisition, Investigation, Methodology, Writing – original draft, Writing – review & editing.

Funding

The author(s) declare financial support was received for the research, authorship, and/or publication of this article. This work has been funded by ANR BIOPSIS project, grant ANR-16-CE-0002–01 of the French Agence Nationale de la Recherche. This work was partially supported by ISblue project, Interdisciplinary graduate school for the blue planet (ANR-17-EURE-0015) and co-funded by a grant from the French government under the program "Investissements d'Avenir" embedded in France 2030.

Acknowledgments

The authors gratefully acknowledge the technical support of M. Le Goff(1) and M. Gallinari(1) through the analytical platform PACHIDERM.

Conflict of interest

Author AG was employed by the company AlgaeNutri.

The remaining authors declare that the research was conducted in the absence of any commercial or financial relationships that could be construed as a potential conflict of interest.

Publisher's note

Supplementary material

The Supplementary Material for this article can be found online at: https://www.frontiersin.org/articles/10.3389/fmars.2024.1331333/full#supplementary-material

SUPPLEMENTARY TABLE 1
Synechococcus contribution to the global Si cycle. The contribution of *Synechococcus* to the annual stocks of bSi was estimated for each of the Longhurst provinces using (1) the *Synechococcus* concentration found in the dataset made available by Visintini et al. (2021), (2) the main *Synechococcus* clade of the different oceanic areas (Zwirglmaier et al., 2008; Tai and Palenik, 2009; Huang et al., 2012; Sohm et al., 2016; Grébert et al., 2018; Doré et al., 2020; Wang et al., 2022; Wei et al., 2022), and (3) the *in situ* and clade specific laboratory measurements of Si *Synechococcus* cellular quotas from this study but also to our acknowledge, those from all other existing studies (Baines et al., 2012; Ohnemus et al., 2016; Brzezinski et al., 2017; Krause et al., 2017; Wei et al., 2022). For the first time in a budget, we also integrated the impact of P and Fe limitations. To do so we assigned a limitation to each Longhurst provinces using Browning and Moore (2023). We used the Si quotas corresponding to the P and Fe limitations when our clades were dominating the corresponding zone, and data measured *in situ* when possible. When no *in-situ* data are available we used the Si content measured for the main clade of the zone without taking into account the limitations. For Si production rates we used our measurements which considers the main nutrient limitations describe by Browning and Moore. When our clades were not one of the main *Synechococcus* observed in the Longhurst area, i.e., mainly in Trade winds domain, we used an average value of the rates measured in our study under the limitation describe by Browning and Moore. This hypothesis may give a good idea of the Si production because production rates were not so much clade specific and resemble the two existing other studies (Brzezinski et al., 2017; Krause et al., 2017).
Description of the different data used to estimate the global contribution to the Si cycle: stocks and production. The exponent indicates the origin of the data from literature while the ** Denotes when the data are issued from this study. * Is used when the definition of the headers is provided below the table. Qsi* (fmol/cell) is the Si quota used in the calculation, estimated as describe above. VSi* (d^{-1}): is the Si uptake used to calculate the global Si production due to *Synechococcus*. estimated as described above. bSi stocks resulting from the equation: bSi = [Syn] * productive depth * surface of the Longhurst region * Qsi With [Syn] the average cell concentration estimated from Visintini et al. (2021). PbSi* is the bSi production due to *Synechococcus*. Calculated using the duration of the productive period (t_{pp}: 9 months (Visintini and Flombaum, 2022), except for polar seas where we used 3.5 months as for diatoms in Tréguer et al. (2021)). PbSi = bSi * VSi *t_{pp}/12 a- Brzezinski et al., 2017; b- Doré et al., 2020; c- Grébert et al., 2022; d- Huang et al., 2012; e- Ohnemus et al., 2016; f-Sohm et al., 2016; g- Tai and Palenik, 2009; h- Tang et al., 2014; i- Wang et al., 2022; j- Wei et al., 2022; k- Zwirglmaier et al., 2007, 2008; L- Robicheau et al., 2022; m- Visintini et al., 2021; Visintini and Flombaum, 2022; n- Browning and Moore, 2023; o- Longhurst et al., 1995.

References

Aminot, A., and Kérouel, R. (2007). *Dosage automatique des nutriments dans les eaux marines* (Ifremer), 187.

Baines, S. B., Twining, B. S., Brzezinski, M. A., Krause, J. W., Vogt, S., Assael, D., et al. (2012). Significant silicon accumulation by marine picocyanobacteria. *Nat. Geosci.* 5, 886–891. doi: 10.1038/ngeo1641

Benedetti, F., Gruber, N., and Vogt, M. (2023). Global gradients in species richness of marine plankton functional groups. *J. Plankton Res.* 45 (6), 832–852. doi: 10.1093/plankt/fbad044

Biard, T., Krause, J. W., Stukel, M. R., and Ohman, M. D. (2018). The significance of giant phaeodarians (Rhizaria) to biogenic silica export in the california current ecosystem. *Glob. Biogeochem. Cycles* 32, 987–1004. doi: 10.1029/2018GB005877

Boutorh, J., Cheize, M., Planquette, H., Shelley, R., Lacan, F., Heimbürger, L. E., et al. (2014). III. 5. Trace elements and their isotopes. *CRUISE REPORT* 67.

Boutorh, J., Moriceau, B., Gallinari, M., Ragueneau, O., and Bucciarelli, E. (2016). Effect of trace metal-limited growth on the postmortem dissolution of the marine diatom Pseudo-nitzschia delicatissima: micronutrient-limited diatom dissolution. *Glob. Biogeochem. Cycles* 30, 57–69. doi: 10.1002/2015GB005088

Brand, L. E. (1991). Minimum iron requirements of marine phytoplankton and the implications for the biogeochemical control of new production. *Limnol. Oceanogr.* 36, 1756–1771. doi: 10.4319/lo.1991.36.8.1756

Browning, T. J., and Moore, C. M. (2023). Global analysis of ocean phytoplankton nutrient limitation reveals high prevalence of co-limitation. *Nat. Commun.* 14 (1), 5014. doi: 10.1038/s41467-023-40774-0

Brzezinski, M. A., Alldredge, A. L., and O'Bryan, L. M. (1997). Silica cycling within marine snow. *Limnol. Oceanogr.* 42, 1706–1713. doi: 10.4319/lo.1997.42.8.1706

Brzezinski, M. A., Baines, S. B., Balch, W. M., Beucher, C. P., Chai, F., Dugdale, R. C., et al. (2011). Co-limitation of diatoms by iron and silicic acid in the equatorial pacific. *Deep Sea Res. Part II: Topical Stud. Oceanography* 58 (3-4), 493–511. doi: 10.1016/j.dsr2.2010.08.005

Brzezinski, M. A., Krause, J. W., Baines, S. B., Collier, J. L., Ohnemus, D. C., and Twining, B. S. (2017). Patterns and regulation of silicon accumulation in *Synechococcus* spp. *J. Phycol* 53, 746–761. doi: 10.1111/jpy.12545

Cariou, T., Macé, E., and Morin, P. (2004). *La série océanographique littorale Estacade de l'Observatoire Océanologique de Roscoff: résultats des observations 1985 – 2002*. Available online at: https://www.researchgate.net/publication/299430343_La_serie_oceanographique_littorale_Estacade_de_l'Observatoire_Oceanologique_de_Roscoff_resultats_des_observations_1985_-_2002.

Churakova, Y., Aguilera, A., Charalampous, E., Conley, D. J., Lundin, D., Pinhassi, J., et al. (2023). Biogenic silica accumulation in picoeukaryotes: Novel players in the marine silica cycle. *Environ. Microbiol. Rep.* 15, 282–290. doi: 10.1111/1758-2229.13144

Cohen, N. R., Ellis, K. A., Lampe, R. H., McNair, H., Twining, B. S., Maldonado, M. T., et al. (2017). Diatom transcriptional and physiological responses to changes in iron bioavailability across ocean provinces. *Front. Mar. Sci.* 4. doi: 10.3389/fmars.2017.00360

De Martini, F., and Neuer, S. (2016). From grazer control to carbon export: contrasting the role of synechococcus and prochlorococcus in the sargasso sea. *Am. Geophysical Union* 2016, B31A–B302.

Doré, H., Farrant, G. ,. K., Guyet, U., Haguait, J., Humily, F., Ratin, M., et al. (2020). Evolutionary mechanisms of long-term genome diversification associated with niche partitioning in marine picocyanobacteria. *Front. Microbiol.* 11, 23. doi: 10.3389/fmicb.2020.567431

Doré, H., Guyet, U., Leconte, J., Farrant, G. K., Alric, B., and Garczarek, L. (2023). Differential global distribution of marine picocyanobacteria gene clusters reveals distinct niche-related adaptive strategies. *ISME J.* 17 (5), 720–732. doi: 10.1038/s41396-023-01386-0

Doré, H., Leconte, J., Guyet, U., Breton, S., Farrant, G. K., Demory, D., et al. (2022). Global phylogeography of marine synechococcus in coastal areas reveals strong community shifts. *Msystems* 7 (6), e00656–e00622. doi: 10.1128/msystems.00656-22

Duhamel, S., Kim, E., Sprung, B., and Anderson, O. R. (2019). Small pigmented eukaryotes play a major role in carbon cycling in the P-depleted western subtropical North Atlantic, which may be supported by mixotrophy. *Limnol. Oceanogr.* 64, 2424–2440. doi: 10.1002/lno.11193

Dutkiewicz, S., Morris, J. J., Follows, M. J., Scott, J., Levitan, O., Dyhrman, S. T., et al. (2015). Impact of ocean acidification on the structure of future phytoplankton communities. *Nat. Clim. Change* 5, 1002–1006. doi: 10.1038/nclimate2722

Flombaum, P., Gallegos, J. L., Gordillo, R. A., Rincón, J., Zabala, L. L., Jiao, N., et al. (2013). Present and future global distributions of the marine Cyanobacteria *Prochlorococcus* and *Synechococcus*. *Proc. Natl. Acad. Sci.* 110, 9824–9829. doi: 10.1073/pnas.1307701110

Flombaum, P., and Martiny, A. C. (2021). Diverse but uncertain responses of picophytoplankton lineages to future climate change. *Limnol. Oceanogr.* 66, 4171–4181. doi: 10.1002/lno.11951

George, J. A., Lonsdale, D. J., Merlo, L. R., and Gobler, C. J. (2015). The interactive roles of temperature, nutrients, and zooplankton grazing in controlling the winter-spring phytoplankton bloom in a temperate, coastal ecosystem, Long Island Sound: Long Island Sound winter-spring bloom. *Limnol. Oceanogr.* 60, 110–126. doi: 10.1002/lno.10020

Gobler, C. J., Buck, N. J., Sieracki, M. E., and Sañudo-Wilhelmy, S. A. (2006). Nitrogen and silicon limitation of phytoplankton communities across an urban estuary: The East River-Long Island Sound system. *Est. Coast. Sh. Sci.* 68, 127–138. doi: 10.1016/j.ecss.2006.02.001

Grébert, T., Doré, H., Partensky, F., Farrant, G. K., Boss, E. S., Picheral, M., et al. (2018). Light color acclimation is a key process in the global ocean distribution of *Synechococcus* cyanobacteria. *Proc. Natl. Acad. Sci.* 115, E2010–E2019. doi: 10.1073/pnas.1717069115

Henson, S. A., Sanders, R., and Madsen, E. (2012). Global patterns in efficiency of particulate organic carbon export and transfer to the deep ocean: export and transfer efficiency. *Glob. Biogeochem. Cycles* 26, GB1028. doi: 10.1029/2011GB004099

Huang, S., Wilhelm, S. W., Harvey, H. R., Taylor, K., Jiao, N., and Chen, F. (2012). Novel lineages of *Prochlorococcus* and *Synechococcus* in the global oceans. *ISME J.* 6, 285–297. doi: 10.1038/ismej.2011.106

Krause, J. W., Brzezinski, M. A., Baines, S. B., Collier, J. L., Twining, B. S., and Ohnemus, D. C. (2017). Picoplankton contribution to biogenic silica stocks and production rates in the Sargasso Sea. *Glob. Biogeochem. Cycles* 31, 762–774. doi: 10.1002/2017GB005619

Lasbleiz, M., Leblanc, K., Blain, S., Ras, J., Cornet-Barthaux, V., Hélias Nunige, S., et al. (2014). Pigments, elemental composition (C, N, P, and Si), and stoichiometry of particulate matter in the naturally iron fertilized region of Kerguelen in the Southern Ocean. *Biogeosciences* 11, 5931–5955. doi: 10.5194/bg-11-5931-2014

Leblanc, K., Arístegui, J., Armand, L., Assmy, P., Beker, B., Bode, A., et al. (2012). A global diatom database–abundance, biovolume and biomass in the world ocean. *Earth Syst. Sci. Data* 4 (1), 149–165. doi: 10.5194/essd-4-149-2012

Leblanc, K., Cornet, V., Rimmelin-Maury, P., Grosso, O., Hélias-Nunige, S., Brunet, C., et al. (2018). Silicon cycle in the tropical South Pacific: contribution to the global Si cycle and evidence for an active pico-sized siliceous plankton. *Biogeosciences* 15, 5595–5620. doi: 10.5194/bg-15-5595-2018

Letscher, R. T., Moore, J. K., Martiny, A. C., and Lomas, M. W. (2023). Biodiversity and stoichiometric plasticity increase pico-phytoplankton contributions to marine net primary productivity and the biological pump. *Glob. Biogeochem. Cycles* 37, e2023GB007756. doi: 10.1029/2023GB007756

Leynaert, A., Tréguer, P., Nelson, D. M., and Del Amo, Y. (1996). "32Si as a tracer of biogenic silica production: methodological improvements," in *Integrated marine system analysis. european network for integrated marine system analysis. FWO vlaanderen: minutes of the first network meeting (Brugge, 29.02.96-02.03.96)*. Ed. J. Baeyens, et al, 29–35.

Li, W. K. W. (1998). Annual average abundance of heterotrophic bacteria and *Synechococcus* in surface ocean waters. *Limnol. Oceanogr.* 43, 1746–1753. doi: 10.4319/lo.1998.43.7.1746

Llopis Monferrer, N. L. (2020). Unveiling the role of Rhizaria in the silicon cycle. Université de Bretagne occidentale - Brest. English. ⟨NNT: 2020BRES0041⟩.

Llopis Monferrer, N., Boltovskoy, D., Tréguer, P., Sandin, M. M., Not, F., and Leynaert, A. (2020). Estimating biogenic silica production of rhizaria in the global ocean. *Glob. Biogeochem. Cycles* 34, e2019GB006286. doi: 10.1029/2019GB006286

Longhurst, A., Sathyendranath, S., Platt, T., and Caverhill, C. (1995). An estimate of global primary production in the ocean from satellite radiometer data. *J. Plankton Res.* 17, 1245–1271. doi: 10.1093/plankt/17.6.1245

MaChado, K. B., Vieira, L. C. G., and Nabout, J. C. (2019). Predicting the dynamics of taxonomic and functional phytoplankton compositions in different global warming scenarios. *Hydrobiologia* 830, 115–134. doi: 10.1007/s10750-018-3858-7

Marchetti, A., and Harrison, P. J. (2007). Coupled changes in the cell morphology and the elemental (C, N, and Si) composition of the pennate diatom *Pseudo-nitzschia* due to iron deficiency. *Limnol. Oceanogr.* 52, 2270–2284. doi: 10.4319/lo.2007.52.5.2270

Marinov, I., Doney, S. C., Lima, I. D., Lindsay, K., Moore, J. K., and Mahowald, N. (2013). North-South asymmetry in the modeled phytoplankton community response to climate change over the 21st century. *Glob. Biogeochem. Cycles* 27, 1274–1290. doi: 10.1002/2013GB004599

Marron, A. O., Ratcliffe, S., Wheeler, G. L., Goldstein, R. E., King, N., Not, F., et al. (2016). The evolution of silicon transport in eukaryotes. *Mol. Biol. Evol.* 33, 3226–3248. doi: 10.1093/molbev/msw209

Martin-Jézéquel, V., Hildebrand, M., and Brzezinski, M. A. (2000). Silicon metabolism in diatoms: implications for growth. *J. Phycol.* 36, 821–840. doi: 10.1046/j.1529-8817.2000.00019.x

Moore, C. M., Mills, M. M., Arrigo, K. R., Berman-Frank, I., Bopp, L., Boyd, P. W., et al. (2013). Processes and patterns of oceanic nutrient limitation. *Nat. Geosci.* 6, 701–710. doi: 10.1038/ngeo1765

Moriceau, B., Garvey, M., Ragueneau, O., and Passow, U. (2007). Evidence for reduced biogenic silica dissolution rates in diatom aggregates. *Mar. Ecol. Prog. Ser.* 333, 129–142. doi: 10.3354/meps333129

Muñoz-Marín, M. C., Gómez-Baena, G., López-Lozano, A., Moreno-Cabezuelo, J. A., Díez, J., and García-Fernández, J. M. (2020). Mixotrophy in marine picocyanobacteria: use of organic compounds by *Prochlorococcus* and *Synechococcus*. *ISME J.* 14, 1065–1073. doi: 10.1038/s41396-020-0603-9

Nelson, D. M., Riedel, G. F., Millan-Nunez, R., and Lara-Lara, J. R. (1984). Silicon uptake by algae with no known Si requirement. I. True cellular uptake and pH-induced precipitation by *phaeodactylum tricornutum* (bacillariophyceae) and *platymonas* sp.(prasinophyceae) 1. *J. Phycol.* 20, 141–147. doi: 10.1111/j.0022-3646.1984.00141.x

Ohnemus, D. C., Krause, J. W., Brzezinskid, M. A., Colliere, J. L., Baines, S. B., and Twining, B. S. (2018). The chemical form of silicon in marine *Synechococcus*. *Mar.Chem.* 206, 44–51. doi: 10.1016/j.marchem.2018.08.004

Ohnemus, D. C., Rauschenberg, S., Krause, J. W., Brzezinski, M. A., Collier, J. L., Geraci-Yee, S., et al. (2016). Silicon content of individual cells of *Synechococcus* from the North Atlantic Ocean. *Mar. Chem.* 187, 16–24. doi: 10.1016/j.marchem.2016.10.003

Petrucciani, A., Knoll, A. H., and Norici, A. (2022). Si Decline and diatom evolution: Insights from physiological experiments. *Front. Mar. Sci.* 9, 924452. doi: 10.3389/fmars.2022.924452

Poulton, A. J., Sanders, R., Holligan, P. M., Stinchcombe, M. C., Adey, T. R., Brown, L., et al. (2006). Phytoplankton mineralization in the tropical and subtropical Atlantic Ocean. *Glob. Biogeochem. Cycles* 20 (4). doi: 10.1029/2006GB002712

Price, N. M., Harrison, G. I., Hering, J. G., Hudson, R. J., Nirel, P. M. V., Palenik, B., et al. (1989). Preparation and chemistry of the artificial algal culture medium Aquil. *Biol. Oceanogr.* 6, 443–461. doi: 10.1080/01965581.1988.10749544

Richardson, T. L., and Jackson, G. A. (2007). Small phytoplankton and carbon export from the surface ocean. *Science* 315, 838–840. doi: 10.1126/science.1133471

Robicheau, B. M., Tolman, J., Bertrand, E. M., and LaRoche, J. (2022). Highly-resolved interannual phytoplankton community dynamics of the coastal northwest atlantic. *ISME Commun.* 2 (1), 38.

Siegel, D. A., DeVries, T., Cetinić, I., and Bisson, K. M. (2023). Quantifying the ocean's biological pump and its carbon cycle impacts on global scales. *Annu. Rev. Mar. Sci.* 15, 329–356. doi: 10.1146/annurev-marine-040722-115226

Sohm, J. A., Ahlgren, N. A., Thomson, Z. J., Williams, C., Moffett, J. W., Saito, M. A., et al. (2016). Co-occurring synechococcus ecotypes occupy four major oceanic regimes defined by temperature, macronutrients and iron. *ISME J.* 10 (2), 333–345. doi: 10.1038/ismej.2015.115

Sournia, A., and Birrien, J. L. (1995). La série océanographique côtière de Roscoff (Manche occidentale) de 1985 à 1992. *Cahiers Biologie Mar.* 36, 1–8.

Tai, V., and Palenik, B. (2009). Temporal variation of *Synechococcus* clades at a coastal Pacific Ocean monitoring site. *ISME J.* 3, 903–915. doi: 10.1038/ismej.2009.35

Tang, T., Kisslinger, K., and Lee, C. (2014). Silicate deposition during decomposition of cyanobacteria may promote export of picophytoplankton to the deep ocean. *Nat. Commun.* 5 (1), 4143. doi: 10.1038/ncomms5143

Tostevin, R., Snow, J. T., Zhang, Q., Tosca, N. J., and Rickaby, R. E. M. (2021). The influence of elevated SiO_2(aq) on intracellular silica uptake and microbial metabolism. *Geobiology* 19, 421–433. doi: 10.1111/gbi.12442

Tréguer, P., Bowler, C., Moriceau, B., Dutkiewicz, S., Gehlen, M., Aumont, O., et al. (2018). Influence of diatom diversity on the ocean biological carbon pump. *Nat. Geosci.* 11, 27–37. doi: 10.1038/s41561-017-0028-x

Tréguer, P., Lindner, L., van Bennekom, A. J., Leynaert, A., Panouse, M., and Jacques, G. (1991). Production of biogenic silica in the weddell-scotia seas measured with 32Si. *Limnol. Oceanogr.* 36 (6), 1217–1227. doi: 10.4319/lo.1991.36.6.1217

Tréguer, P. J., Sutton, J. N., Brzezinski, M., Charette, M. A., Devries, T., Dutkiewicz, S., et al. (2021). Reviews and syntheses: the biogeochemical cycle of silicon in the modern ocean. *Biogeosciences* 18 (4), 1269–1289. doi: 10.5194/bg-2020–274

Visintini, N., and Flombaum, P. (2022). Picophytoplankton phenology in the global ocean assessed by quantitative niche models. *Mar. Biol.* 169 (7), 93. doi: 10.1007/s00227-022-04080-5

Visintini, N., Martiny, A. C., and Flombaum, P. (2021). *Prochlorococcus*, *Synechococcus*, and picoeukaryotic phytoplankton abundances in the global ocean. *Limnol. Oceanogr. Lett.* 6, 207–215. doi: 10.1002/lol2.10188

Wang, T., Chen, X., Li, J., and Qin, S. (2022). Distribution and phenogenetic diversity of synechococcus in the bohai sea, china. *J. Oceanology Limnology* 40 (2), 592–604.

Wei, Y., Qu, K., Cui, Z., and Sun, J. (2023). Picocyanobacteria–a non-negligible group for the export of biomineral silica to ocean depth. *J. Environ. Manage.* 342, 118313. doi: 10.1016/j.jenvman.2023.118313

Wei, Y., Sun, J., Li, L., and Cui, Z. (2022). *Synechococcus* silicon accumulation in oligotrophic oceans. *Limnol. Oceanogr.* 67, 552–566. doi: 10.1002/lno.12015

Wilken, S., Hoffmann, B., Hersch, N., Kirchgessner, N., Dieluweit, S., Rubner, W., et al. (2011). Diatom frustules show increased mechanical strength and altered valve morphology under iron limitation. *Limnol. Oceanogr.* 56, 1399–1410. doi: 10.4319/lo.2011.56.4.1399

Zwirglmaier, K., Jardillier, L., Ostrowski, M., Mazard, S., Garczarek, L., Vaulot, D., et al. (2008). Global phylogeography of marine synechococcus and prochlorococcus reveals a distinct partitioning of lineages among oceanic biomes. *Environ. Microbiol.* 10 (1), 147–161. doi: 10.1111/j.1462-2920.2007.01440.x